Applied Mathematics & Information Sciences
An International Journal

http://dx.doi.org/10.12785/amis/080420

Mathematical Models of 3D Magnetic Field and 3D Positioning System by Magnetic Field

Dong Lin[*] *and Xin Chen*

College of Physics and Information Engineering, Fuzhou University, Fuzhou, Fujian, P. R. China

Received: 21 Jul. 2013, Revised: 23 Oct. 2013, Accepted: 24 Oct. 2013
Published online: 1 Jul. 2014

Abstract: A practical 3D positioning system was developed based on the mathematical models of 3D magnetic field induced by a single loop coil. Mathematical expression of the magnetic intensity in 3D space was derived in detail. 3D positioning using magnetic field provides a new approach to detect the location of a non-visible target inside a non-magnet-shielded object such as human body by taking advantage of penetrative capability of magnetic field through such object. By attaching magnetic sensor to medical instruments, the signals generated by the sensor inside the body response to the magnetic field produced by emitter coils outside body are analyzed to determine the location of sensor as well as the position of the medical instrument. Real-time six-degree freedom measurement for 3D magnetic sensor and five-degree freedom measurement for single magnetic sensor were realized. This system provides a new approach to determine the 3D position and orientation of endoscope inside the patient's body by harmless magnetic field.

Keywords: 3D positioning, mathematical models, magnetic field, sensor, endoscope

1 Introduction

3D positioning using magnetic field provides a new approach to detect the location of a non-visible target inside a non-magnet-shielded object such as human body by taking advantage of penetrative capability of magnetic field through such object. The potential application of this technology in medical care is tremendous. It's more safe and easy to operate than traditional X-ray penetration positioning and ultrasonic positioning. By attaching magnetic sensor to medical instruments (for instance, endoscope), the signals generated by the sensor inside the body response to the magnetic field produced by emitter coils outside body are analyzed to determine the location of sensor as well as the position of the medical instrument.

2 Mathematic Model of Magnetic Field in 3D Space

The accuracy of magnetic fields generated by current coil is the highest one. Magnetic intensity can be accurately derived based on Biot-Savart principle [1]. Regarding to computation complexity and manufacturing, the loop coil with axis symmetry is actually ideal.

In the analysis of magnetic field, the winding of coil can be neglected and the coil can be considered as an ideal circular loop. The computation error from such approximation is less than 5ppm which is acceptable in most situations. Moreover, the amount of computation is greatly reduced.

*2.1 Magnetic Induction at a Given Point Produced by Current Element Id**l***

A given point magnetic intensity produced by current element $Id\boldsymbol{l}$ is calculated according to Biot-Savart principle,

$$d\boldsymbol{B} = \frac{\mu_0 Id\boldsymbol{l} \times \boldsymbol{r}}{4\pi r^3}, \tag{1}$$

where $\boldsymbol{r}$ is the vector from current element to the given point. $\boldsymbol{B}$ can be obtained by integral,

$$\boldsymbol{B} = \nabla \times \left[\frac{\mu_0}{4\pi}\int \frac{Id\boldsymbol{l}}{r}\right] = \nabla \times \boldsymbol{A}, \tag{2}$$

where

$$\boldsymbol{A} = \frac{\mu_0}{4\pi}\int \frac{Id\boldsymbol{l}}{r}, \tag{3}$$

[*] Corresponding author e-mail: lindong@fzu.edu.cn

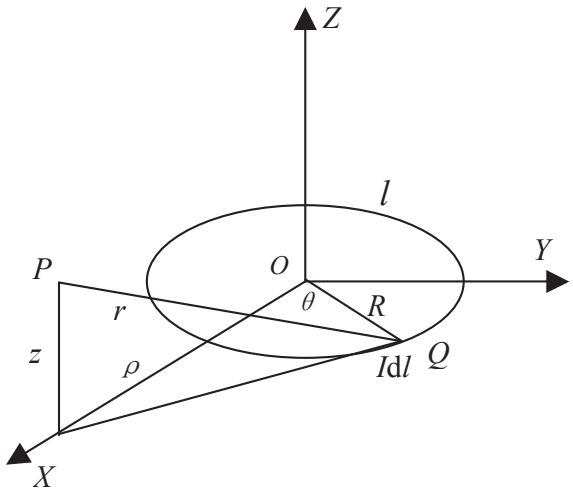

Fig. 1: Magnetic induction produced by a single loop coil.

$\boldsymbol{A}$ is the vector potential of magnetic field. Usually when the field distributing is known and $\boldsymbol{A}$ is calculated first, then $\boldsymbol{B}$ can be conveniently obtained by (2).

2.2 Magnetic Induction at a Given Point Produced by Single Loop Coil with Current

Single circular loop carrying line current is most simple in shape. Magnetic field produced by loop coil with current depends on radius of coil and current in the coil. It is easy to calculate the magnetic induction at axis of coil, and elliptic integral would be needed to calculate the Magnetic intensity at a given point away from axis [2].

For a loop coil of radius R with current I located in XOY plane in rectangular coordinates with O being the centre of the circle, $P(x,y,z)$ being the given point, and $\boldsymbol{l}$ being the loop current, as shown in Fig. 1, $\mathrm{d}\boldsymbol{l}$ is defined as differential of coil tangent vector at point $Q(x',y',z')$ with the direction same as current. The $\boldsymbol{r}$ is defined as the vector from Q to P.

$$\mathrm{d}\boldsymbol{l} = \mathrm{d}x'\boldsymbol{i} + \mathrm{d}y'\boldsymbol{j} + \mathrm{d}z'\boldsymbol{k}. \tag{4}$$

$$r = \sqrt{(x-x')^2 + (y-y')^2 + (z-z')^2}. \tag{5}$$

For the convenience of computation cylindrical coordinates are adopted since magnetic field produced by loop current has axis symmetry. It can be assumed, without loss of generality that the given point P locates at $(\rho,0,z)$ in XOZ plane. A vector from any point at loop coil $Q(R\cos\theta, R\sin\theta, 0)$ to point P is

$$\boldsymbol{r}(Q,P) = (\rho - R\cos\theta)\boldsymbol{i} + (0 - R\sin\theta)\boldsymbol{j} + (z-0)\boldsymbol{k}. \tag{6}$$

The length of vector,

$$\begin{aligned} r(Q,P) &= \sqrt{(\rho - R\cos\theta)^2 + (0 - R\sin\theta)^2 + (z-0)^2} \\ &= \sqrt{\rho^2 + R^2 + z^2 - 2\rho R\cos\theta}. \end{aligned} \tag{7}$$

In cylindrical coordinates, (4) can be described as

$$\mathrm{d}\boldsymbol{l} = R(-\sin\theta e_\theta + \cos\theta e_\theta)\,\mathrm{d}\theta. \tag{8}$$

In which e_θ is circumference unit vector at point $Q(x',y',z')$. Thus $\boldsymbol{A}$ in (3) can be rewritten as

$$\boldsymbol{A}(\rho,0,z) = \frac{\mu_0}{4\pi}\int_0^{2\pi} \frac{IR(-\sin\theta e_\theta + \cos\theta e_\theta)\,\mathrm{d}\theta}{\sqrt{\rho^2 + R^2 + z^2 - 2\rho R\cos\theta}}, \tag{9}$$

in which integral result containing $\sin\theta$ equals to zero since $\sin\theta$ is odd function about θ, and $\cos\theta$ is even function about θ. Let $\theta = \pi - 2\alpha$, then

$$\cos\theta\,\mathrm{d}\theta = 2\left(2\sin^2\alpha - 1\right)\mathrm{d}\alpha, \tag{10}$$

and (9) is simplified as

$$\begin{aligned} \boldsymbol{A}(\rho,0,z) = \frac{\mu_0 IR}{\pi}\int_0^{\frac{\pi}{2}} &\frac{\left(2\sin^2\alpha - 1\right)}{\sqrt{(\rho+R)^2 + z^2}} \\ &\cdot \frac{1}{\sqrt{1 - \frac{4\rho R}{(\rho+R)^2+z^2}\sin^2\alpha}}\mathrm{d}\alpha \cdot e_\theta. \end{aligned} \tag{11}$$

Let

$$k = \sqrt{\frac{4\rho R}{(\rho+R)^2 + z^2}}, \tag{12}$$

$$\int_0^{\frac{\pi}{2}} \frac{\mathrm{d}\alpha}{\sqrt{1 - k^2\sin^2\alpha}} = K(k), \tag{13}$$

$$\int_0^{\frac{\pi}{2}} \sqrt{1 - k^2\sin^2\alpha}\,\mathrm{d}\alpha = E(k), \tag{14}$$

then (11) is simplified as

$$\boldsymbol{A}(\rho,0,z) = \frac{\mu_0 I}{\pi k}\sqrt{\frac{R}{\rho}}\left[\left(1 - \frac{k^2}{2}\right)K(k) - E(k)\right]\cdot e_\theta, \tag{15}$$

where $K(k)$ and $E(k)$ are complete elliptic integrals of the first and second kinds, and $\boldsymbol{A}$ is vector potential of loop coil with current. $\boldsymbol{B}$ is obtained by calculating the rotation of $\boldsymbol{A}$ according to (2). Differential formula of complete elliptic integrals of the first and second kinds would be employed when calculating the rotation.

$$\frac{\mathrm{d}}{\mathrm{d}k}K(k) = \frac{E(k)}{k(1-k^2)} - \frac{K(k)}{k}, \tag{16}$$

$$\frac{\mathrm{d}}{\mathrm{d}k}E(k) = \frac{E(k) - K(k)}{k}. \tag{17}$$

Rotation in cylindrical coordinates is represented as

$$\nabla \times \mathbf{A} = \left(\frac{1}{\rho}\cdot\frac{\partial A_z}{\partial \theta} - \frac{\partial A_\theta}{\partial z}\right)e_\rho + \left(\frac{\partial A_\rho}{\partial z} - \frac{\partial A_z}{\partial \rho}\right)e_\theta + \frac{1}{\rho}\left[\frac{\partial}{\partial \rho}(\rho A_\theta) - \frac{\partial A_\rho}{\partial \theta}\right]e_z. \quad (18)$$

B_ρ, B_θ, B_Z can be found by

$$B_\rho = \frac{1}{\rho}\cdot\frac{\partial A_z}{\partial \theta} - \frac{\partial A_\theta}{\partial z} = -\frac{\partial A_\theta}{\partial z} = -\frac{\partial A_\theta}{\partial k}\cdot\frac{\partial k}{\partial z} = \frac{\mu_0 I}{2\pi}\cdot\frac{z}{\rho}\cdot\frac{-K(k) + \frac{R^2+\rho^2+z^2}{(R-\rho)^2+z^2}\cdot E(k)}{\sqrt{(R+\rho)^2+z^2}}, \quad (19)$$

$$B_\theta = \frac{\partial A_\rho}{\partial z} - \frac{\partial A_z}{\partial \rho} = 0, \quad (20)$$

$$B_Z = \frac{1}{\rho}\left[\frac{\partial}{\partial \rho}(\rho A_\theta) - \frac{\partial A_\rho}{\partial \theta}\right] = \frac{1}{\rho}\frac{\partial(\rho A_\theta)}{\partial \rho} = \frac{A_\theta}{\rho} + \frac{\partial A_\theta}{\partial \rho} = \frac{\mu_0 I}{2\pi}\cdot\frac{K(k) + \frac{R^2-\rho^2-z^2}{(R-\rho)^2+z^2}\cdot E(k)}{\sqrt{(R+\rho)^2+z^2}}. \quad (21)$$

Rectangular coordinates are convenient in actual application. To obtain the magnetic induction intensity $\boldsymbol{B}$ of a arbitrary given point $P(x,y,z)$ around the loop coil, firstly the rectangular coordinates were converted into circular cylindrical coordinates $P(\rho,\theta,z)$. The components of $\boldsymbol{B}$ in circular cylindrical coordinates were then calculated with (19), (20) and (21), and converted back to rectangular coordinates, which include three components (Bx, By, Bz). The above procedure is expressed as

$$\boldsymbol{B} = f[P(x,y,z)]. \quad (22)$$

2.3 Magnetic Field Produced by Three Loop Coils Orthogonal to Each Other

As shown in Fig. 2, three circular coils are orthogonal to each other. The axis of these three coils coordinate with axis X, Y and Z respectively. The relationship between direction of the coil current and positive direction of the coordinate axis obeys the right-hand-screw principle. The magnetic field is emitted by three coils in turn with a certain period under the control of the sequential circuit.

Since three coils work in time division mode, the magnetic field produced by each coil coincides in the same single loop coil, but is different with the direction of the axis. The method of using revolving coordinates is presented in [2]. According to the computation model of single loop coil Z, we can easily derive the formula of the magnetic induction intensity ***BX*** and ***BY*** for coil X and Y

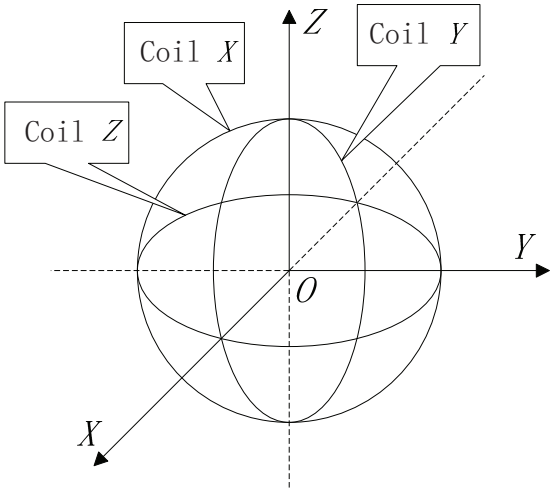

Fig. 2: Structure of three emitting coils.

at any give point $P(x,y,z)$ in the surrounding space. It can be expressed as

$$\begin{cases} \boldsymbol{BX} = f[P(x,y,z)\cdot T_y(-90^\circ)]\cdot T_y(90^\circ), \\ \boldsymbol{BY} = f[P(x,y,z)\cdot T_x(90^\circ)]\cdot T_x(-90^\circ), \\ \boldsymbol{BZ} = f[P(x,y,z)], \end{cases} \quad (23)$$

where $Tx(\cdot)$ and $Ty(\cdot)$ represent the angular rotation around the *X-axis* and *Y-axis* according to right-hand-screw rule. ***BX*** includes three components (BXx, BXy, BXz), ***BY*** includes three components (BYx, BYy, BYz), and ***BZ*** includes three components (BZx, BZy, BZz).

3 Realization of Six-degree Freedom Positioning Using 3D Magnetic Sensor

Three orthogonal coils compose of 3D magnetic sensor for the convenience of mathematical analysis. The shape of 3D magnetic sensor is similar to the emitting coils, but the size is much smaller. In a practical system some other type of sensors such as MR may be chosen. The orientation of 3D magnetic sensor (tip) is described by its relative position to the emitting coils coordinates. The orientation reference frame is obtained by moving the base reference frame of the emitting coils to point P. The orientation of 3D sensor is represented by orientation (a,b,c), and it is obtained by the angular rotation of *a-angle*, *b-angle* and *c-angle* around the *x-axis*, *y-axis* and *z-axis* in turn according to the orientation reference frame. A tip with different orientation (a,b,c) results in induce different components of ***BX***, ***BY***, ***BZ***. Magnetic

intensity induced by the tip with orientation (a,b,c) is described as

$$\begin{cases} \boldsymbol{BX}' = \boldsymbol{BX}\cdot T_x(-a)\cdot T_y(-b)\cdot T_z(-c) \\ \quad = f[P(x,y,z)\cdot T_y(-90^\circ)]\cdot T_y(90^\circ) \\ \quad \cdot T_x(-a)\cdot T_y(-b)\cdot T_z(-c), \\ \boldsymbol{BY}' = \boldsymbol{BY}\cdot T_x(-a)\cdot T_y(-b)\cdot T_z(-c) \\ \quad = f[P(x,y,z)\cdot T_x(90^\circ)]\cdot T_x(-90^\circ) \\ \quad \cdot T_x(-a)\cdot T_y(-b)\cdot T_z(-c), \\ \boldsymbol{BZ}' = \boldsymbol{BZ}\cdot T_x(-a)\cdot T_y(-b)\cdot T_z(-c) \\ \quad = f[P(x,y,z)]\cdot T_x(-a)\cdot T_y(-b)\cdot T_z(-c). \end{cases} \tag{24}$$

The angular rotation is negative since the rotated object is the tip coordinates. In practical system, $\boldsymbol{BX}'(BX'x,\ BX'y,\ BX'z)$, $\boldsymbol{BY}'(BY'x,\ BY'y,\ BY'z)$, $\boldsymbol{BZ}'(BZ'x,\ BZ'y,\ BZ'z)$ are obtained first, and then a nonlinear equation group with position (x,y,z) and orientation (a,b,c) as variables can be established. Six-degree freedom positioning can be realized by solving the equation group using optimization to obtain a group of data (x,y,z,a,b,c) which corresponds to the receiving signals.

4 "Position First, Orientation After" Two-step Method

Though the results can be derived by solving the set of nonlinear equations with six unknowns directly, the computation complexity is really high. The method called "Position First, Orientation After" is proposed. It converts the issue from directly solving six unknowns to successively solving every three unknowns in proper order. It can be known from (24) that $\boldsymbol{BX}'$, $\boldsymbol{BY}'$ and $\boldsymbol{BZ}'$ are the vector $\boldsymbol{BX}$, $\boldsymbol{BY}$ and $\boldsymbol{BZ}$ after rotation, respectively, so

$$\begin{cases} |\boldsymbol{BX}| = |\boldsymbol{BX}'| = \sqrt{BX_x'^2 + BX_y'^2 + BX_z'^2}, \\ |\boldsymbol{BY}| = |\boldsymbol{BY}'| = \sqrt{BY_x'^2 + BY_y'^2 + BY_z'^2}, \\ |\boldsymbol{BZ}| = |\boldsymbol{BZ}'| = \sqrt{BZ_x'^2 + BZ_y'^2 + BZ_z'^2}. \end{cases} \tag{25}$$

When $(BX'x,\ BX'y,\ BX'z)$, $(BY'x,\ BY'y,\ BY'z)$, $(BZ'x,\ BZ'y,\ BZ'z)$ are measured, they are substituted in (25), to calculate the results of $|\boldsymbol{BX}|$, $|\boldsymbol{BY}|$ and $|\boldsymbol{BZ}|$.

$|\boldsymbol{BX}|$, $|\boldsymbol{BY}|$ and $|\boldsymbol{BZ}|$ have nothing to do with the tip orientation (a,b,c), but only relate to the tip position (x,y,z). Modulus operations are done for both sides of (23), then

$$\begin{cases} |\boldsymbol{BX}| = \left| f[P(x,y,z)\cdot T_y(-90^\circ)]\cdot T_y(90^\circ) \right|, \\ |\boldsymbol{BY}| = |f[P(x,y,z)\cdot T_x(90^\circ)]\cdot T_x(-90^\circ)|, \\ |\boldsymbol{BZ}| = |f[P(x,y,z)]|. \end{cases} \tag{26}$$

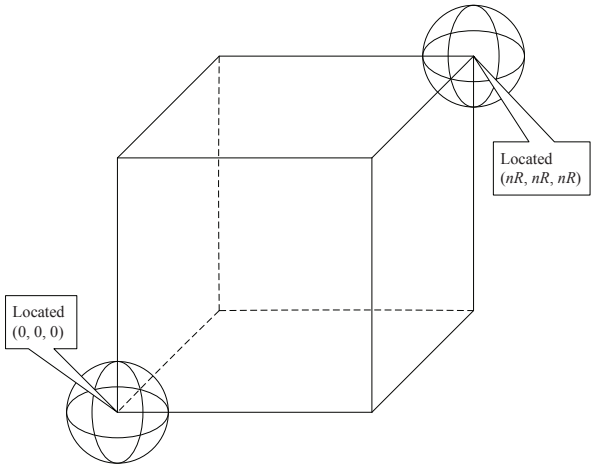

Fig. 3: Structure of two emitting coils groups.

We can search a suitable position (x,y,z) for the set of nonlinear equations with three unknowns in (26). And the solution of the system is achieved by function $fsolve(\ )$ in MATLAB.

When the position (x,y,z) of the tip is determined, it can be substituted in (23), to get the vector $\boldsymbol{BX}$, $\boldsymbol{BY}$, $\boldsymbol{BZ}$. The next step is to confirm the orientation (a,b,c), which makes (24) work. Therefore, (24) converts to a nonlinear equation system with three unknown variables, and the solution of the system is also achieved by the function $fsolve(\ )$ in MATLAB.

5 Realization of Five-degree Freedom Measurement Using Single Magnetic Sensor

Due to limitation of size and installation requirements, single magnetic senor may be needed under certain circumstances. However, only single sensor is not enough for positioning function, because it can detect the intension from one direction. Therefore another group of 3D emitting coils should be needed in the system, and then enough independent equations can be obtained. As shown in Fig. 3, at the diagonal of the cube, there are two groups of 3D emitting coils attached. The second groups of 3D emitting coils are located at (nR,nR,nR) in the coordinates of the first groups of emitting coils. R is the radius of an emitting coil and n can be selected according to the desired workspace, generally between 5 and 10.

The orientation of single magnetic sensor (tip) is described by its axis direction relative to the emitting coils coordinates. Moving the base reference frame of the base emitting coils to point P gives the orientation reference frame. The orientation of single sensor represented by orientation (a,b) is obtained by the

angular rotating *a-angle* and *b-angle* around the *x-axis* and *y-axis* in turn from the original state according to the orientation reference frame. The original state of the tip is defined by its axis direction the same as *z-axis*, just as *z-coil* in 3D sensor. The tip at point $P(x,y,z)$ with different orientation (a,b) results in induce the different components of $BX1$, $BY1$, $BZ1$ and $BX2$, $BY2$, $BZ2$. What the tip induces with orientation (a,b) can be described as

$$BX1'z = f\ [P(x,y,z)\cdot T_y(-90^\circ)]\cdot T_y(90^\circ) \cdot\ T_x(-a)\cdot T_y(-b)\cdot[0,0,1]', \tag{27}$$

$$BY1'z = f\ [P(x,y,z)\cdot T_x(90^\circ)]\cdot T_x(-90^\circ) \cdot\ T_x(-a)\cdot T_y(-b)\cdot[0,0,1]', \tag{28}$$

$$BZ1'z = f\,[P(x,y,z)]\cdot T_x(-a)\cdot T_y(-b)\cdot[0,0,1]', \tag{29}$$

$$BX2'z = f\ [P(x-nR,y-nR,z-nR)\cdot T_y(-90^\circ)] \cdot\ T_y(90^\circ)\cdot T_x(-a)\cdot T_y(-b)\cdot[0,0,1]', \tag{30}$$

$$BY2'z = f\ [P(x-nR,y-nR,z-nR)\cdot T_x(90^\circ)] \cdot\ T_x(-90^\circ)\cdot T_x(-a)\cdot T_y(-b)\cdot[0,0,1]', \tag{31}$$

$$BZ2'z = f\ [P(x-nR,y-nR,z-nR)]\cdot T_x(-a) \cdot\ T_y(-b)\cdot[0,0,1]'. \tag{32}$$

In which matrix $[0,0,1]'$ picks up the z component induced by single magnetic sensor. $BX1'z$, $BY1'z$, $BZ1'z$ are from the first group of emitting coils, and $BX2'z$, $BY2'z$, $BZ2'z$ are from the second group of emitting coils. Then a nonlinear equation group can be established with position (x,y,z) and orientation (a,b) as variables. Five degrees of freedom measurement can be realized by solving the equation group using optimization to obtain a group of data (x,y,z,a,b) which corresponds to the receiving signals.

6 Fast Numerical Computation of Elliptic Integrals

Elliptic integral is encountered when calculating B_ρ and B_z from (19) and (21). MATLAB provides an elliptic integral function *ellipke*( ) to calculate type I and type II elliptic integral, and the computation accuracy is *eps* ($eps = 2.2204\times10^{-16}$ in MATLAB). However, since the recursive formula algorithm is adopted during the computation, the program keeps running until the required *eps* is reached. Therefore, large amounts of computation are needed in this way. In addition, the function is called frequently during the process of calculating, and it means time consuming. So it is necessary to look for a fast algorithm that can meet the request accuracy in engineering practice.

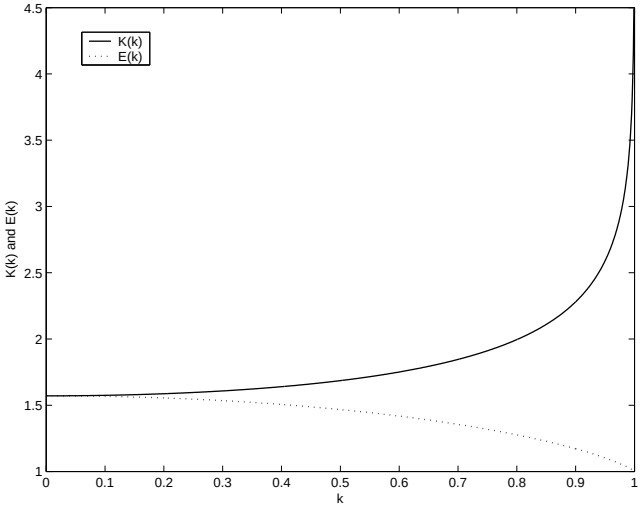

Fig. 4: $K(k)$ and $E(k)$ calculated by using polynomials approximation.

By using polynomials approximation method, a fast numerical computation algorithm for elliptic integral is proposed.

$$K(k) = \sum_{i=0}^{4} a_i t^i - \ln t\cdot\sum_{i=0}^{4} b_i t^i + \varepsilon(k), \tag{33}$$

$$E(k) = 1 + \sum_{i=1}^{4} c_i t^i - \ln t\cdot\sum_{i=1}^{4} d_i t^i + \varepsilon(k), \tag{34}$$

where $t = 1-k^2$. Here the coefficients a_i, b_i, c_i and d_i [3] are

$a_0 = 1.38629436112$, $b_0 = 0.50000000000$,
$a_1 = 0.09666344259$, $b_1 = 0.12498593597$,
$a_2 = 0.03590092383$, $b_2 = 0.06880248576$,
$a_3 = 0.03742563713$, $b_3 = 0.03328355346$,
$a_4 = 0.01451196212$, $b_4 = 0.00441787012$,
$c_1 = 0.44325141463$, $d_1 = 0.24998368310$,
$c_2 = 0.06260601220$, $d_2 = 0.09200180037$,
$c_3 = 0.04757383546$, $d_3 = 0.04069697526$,
$c_4 = 0.01736506451$, $d_4 = 0.00526449639$.

The absolute error $\varepsilon(k)$ is less than 2×10^{-8}. It is fast to use (33) and (34) for elliptic integral computation, and the accuracy can meet the practical requirements. $K(k)$ and $E(k)$ calculated by (33) and (34) are shown in Fig. 4. The calculation errors by polynomial approximation are shown in Fig. 5, comparing with the elliptic integral function provided by MATLAB.

7 3D Positioning System using Magnetic Field

The system configuration is shown in Fig. 6, which consists of emitting control unit, emitting coils, receiving

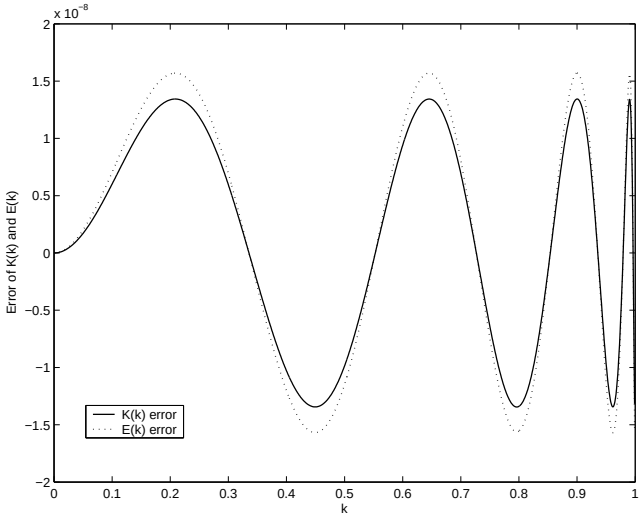

Fig. 5: $K(k)$ and $E(k)$ calculation errors.

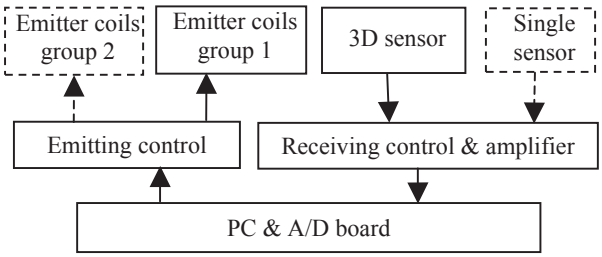

Fig. 6: System configuration.

coils (tip), receiving control unit & amplifier, and PC with A/D board. The controlling unit produces the controlling signal to the whole system and the carrier needed for the emitting magnetic field. Then the carrier is sent to three power amplifiers through CMOS switches. The outputs of amplifiers are sent respectively to the three emitting loop coils working at one by one mode.

The signals from magnetic sensors response to the magnetic field produced by emitter coils are received and amplified by the receiving control & amplifier unit, and after being multiplexed, are narrow-band filtered, synchronously demodulated, low-pass filtered and then sampled and hold. The group of signal corresponding to what is received is converted to digital signal by A/D converter block. Based on model of magnetic field, a nonlinear equation group with position (x,y,z) and orientation (a,b,c) as variables are established and solved to obtain a group of data (x,y,z,a,b,c). A positioning procedure is completed.

A group of 3D emitting coils and 3D magnetic sensor are used to measure six-degree freedom position, and two groups of 3D emitting coils and single magnetic sensor are used while measuring the five-degree freedom position. As shown in Fig. 6, the difference was represented by dashed line. Most of them are the same, but only several differences in the control unit.

8 3D Visualization of Position and Orientation

The position and orientation of a tip can be displayed with a normal three-view drawing with front, side and top views given in orthographic projections or axonometric drawing by MATLAB program. The position (x,y,z) and orientation (a,b,c) of the tip can be displayed conveniently by calling the graphic plot functions in MATLAB. The position (x,y,z) of the tip can be directly displayed in 3D projection plane. In order to show the orientation (a,b,c) of the tip, the unit vectors of the tip coordinate system are used to indicate the directions of the tip coordinate axes.

After using graphic plot function *plot*3( ) to draw 3D graphics, different views can be observed from different viewpoints. Viewpoint of the observer is determined by two parameters, which are *azimuth* angle and *elevation* angle. These can be set by calling the function $view(azimuth, elevation)$ in MATLAB.

The examples of position $(3,1,2)$ and orientation $(10,20,30)$ are shown in Fig. 7, Fig. 8 and Fig. 9, where the results of projecting the 3D graphic on XOZ, YOZ, and XOY planes, namely, setting the $view(0,0)$, $view(90,0)$, and $view(0,90)$, respectively. And an axonometric drawing is shown in Fig. 10, when setting $view(-37.5,30)$.

9 Experiment Results

The radius of emitting coils and receiving coils in the trial system are 17.5cm and 2.5cm respectively. The position and its orientation precision data from our experiments is given in Table 1. And the magnetic equation groups are solved by MATLAB Optimization Toolbox. In addition, the validity of the solution is proved via calculating the theoretical value for any given arbitrary position and orientation.

By the way, since our experimental condition has some limitations, the precision of final results may be rough and can still be improved. When the sensor is near the effective region of the emitting coils, the measured values are very close to theoretical values. But when the sensor is far from the emitting coils, the positioning precision is deteriorated due to much weak induction intensity. Moreover, the precision is also influenced by modeling error, measurement error, truncation error and rounding error etc. and will be improved in the future research.

Both of theoretical analysis and experimental results show that the proposed method is feasible for 3D

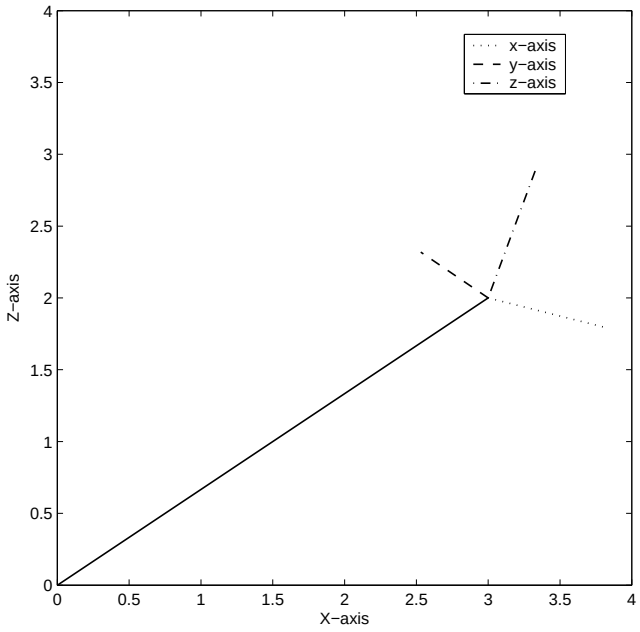

Fig. 7: Positioning results projecting on XOZ plane (Setting $view(0,0)$).

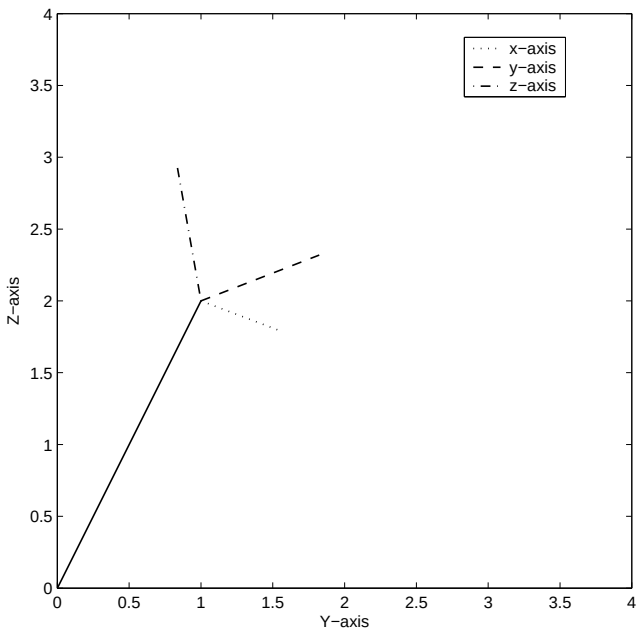

Fig. 8: Positioning results projecting on YOZ plane (Setting $view(90,0)$).

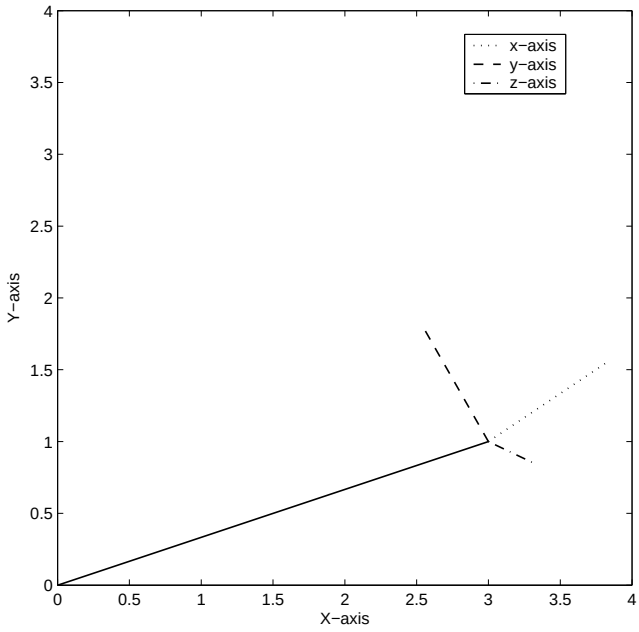

Fig. 9: Positioning results projecting on XOY plane (Setting $view(0,90)$).

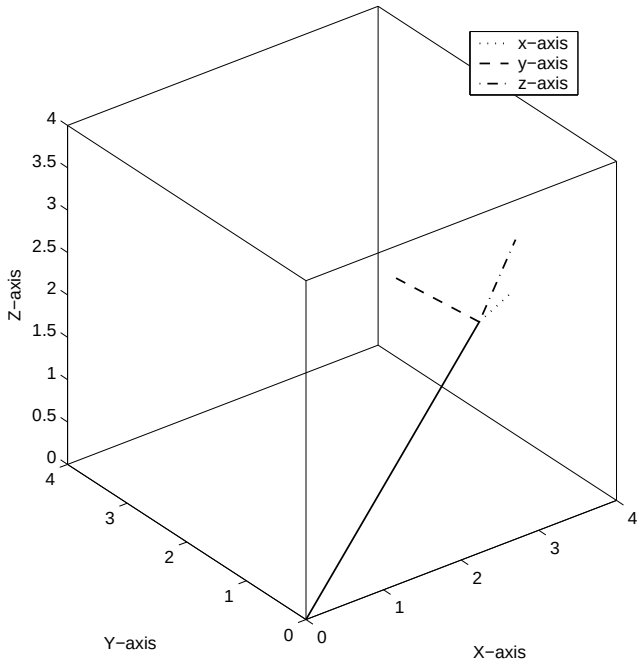

Fig. 10: An axonometric drawing of positioning results (Setting $view(-37.5,30)$).

Table 1: Experiment results.

Distance (mm)	Precision			
	3D magnetic sensor		Single magnetic sensor	
	Position (mm)	Orientation (degree)	Position (mm)	Orientation (degree)
350	< 2	< 3	< 3	< 4
500	< 6	< 7	< 7	< 8
700	< 12	< 14	< 13	< 15

positioning, and the mathematical model can match the physical model well. It is expected to apply the positioning system to determine the location of medical instruments (endoscope) inside the body after further minimization of the tip. The position and orientation of endoscope tip are obtained real-time and added to 3D CT images scanned in advance, as a result, the movement of endoscope tip inside the body can be clearly displayed and navigated thus helping the diagnosis without the negative effects of X-ray to patients and doctors.

Acknowledgement

This paper is supported by XRC Foundation of Fuzhou University, China (No. XRC-1280).

References

[1] Chen Xin, Lin Dong, Zhang Qing-hui, et.al. Three dimensional localization and navigation for endoscopic probe using magnetic field, Chinese Journal of Biomedical Engineering, **21**, 466-470 (2002).

[2] Lin Dong, Chen Xin, Zheng Huiru, Research on determination of the 3D position of endoscope by magnetic field, Proceedings of the International Conference on Sensors and Control Techniques, 343-346 (2000).

[3] Milton Abramowitz, Irene A. Stegun, Handbook of Mathematical Functions, National Bureau of Standards, 591-592 (1964).

Dong Lin received the B.S. degree and M.S. degree from Fuzhou University, Fuzhou, P.R.China, in 1991 and 1999 respectively, and PhD degree from Shanghai Jiaotong University, Shanghai, P.R.China, in 2006. He is currently an Associate Professor with the College of Physics and Information Engineering at Fuzhou University, Fuzhou, China. He has published over 15 papers in journals and international conferences. His research interests are in the areas of mobile communication, mathematical modeling, digital video and image processing.

Xin Chen is a professor of the College of Physics and Information Engineering of Fuzhou University, Fuzhou Fujian P.R.China. He is the member of SPIE and CIE. He has published over 90 papers in journals and international conferences. His research interests are in the areas of image processing, biomedical engineering and computer network.